Modification of Iron(II) Tridentate Bis(imino)pyridine Complexes by a Boryl Group for the Production of α-Olefins at High Temperature[†]

Alex S. Ionkin,* William J. Marshall, Douglas J. Adelman, Barbara Bobik Fones, Brian M. Fish, and Matthew F. Schiffhauer

DuPont Central Research & Development, Experimental Station, Wilmington, Delaware 19880-0328

Received January 14, 2008

A new series of boryl-substituted bis(imino)pyridine ligands [*o*-PinacolB-Ph-N=C(Me)-Py-C(Me)=N-Ph-*o*-BPinacol], Pinacol = (−O-(Me)$_2$C−C(Me)$_2$-O−) (**6**), [2,4,6-tri-Me-Ph-N=C(Me)-Py-C(Me)=N-Ph-*o*-BPinacol] (**11**), [4-bromo-2,6-di-Me-Ph-N=C(Me)-Py-C(Me)=N-Ph-*o*-BPinacol] (**12**), [2,4,6-tri-Me-Ph-N=C(Me)-Py-C(Me)=N-Ph-*m*-BPinacol] (**14**), [2,4,6-tri-Me-Ph-N=C(Me)-Py-C(Me)=N-Ph-*p*-BPinacol] (**17**), and [4-Bromo-2,6-di-Me-Ph-N=C(Me)-Py-C(Me)=N-Ph-*p*-BPinacol] (**18**), and their corresponding Fe(II) complexes [{*o*-PinacolB-Ph-N=C(Me)-Py-C(Me)=N-Ph-*o*-BPinacol}FeCl$_2$] (**3**), [{2,4,6-tri-Me-Ph-N=C(Me)-Py-C(Me)=N-Ph-*o*-BPinacol}FeCl$_2$] (**19**), [{4-bromo-2,6-di-Me-Ph-N=C(Me)-Py-C(Me)=N-Ph-*o*-BPinacol}FeCl$_2$] (**20**), [{2,4,6-tri-Me-Ph-N=C(Me)-Py-C(Me)=N-Ph-*m*-BPinacol}-FeCl$_2$] (**21**), [{2,4,6-tri-Me-Ph-N=C(Me)-Py-C(Me)=N-Ph-*p*-BPinacol}FeCl$_2$] (**22**), and [{4-bromo-2,6-di-Me-Ph-N=C(Me)-Py-C(Me)=N-Ph-*p*-BPinacol}FeCl$_2$] (**23**) were synthesized. According to X-ray analysis, the introduction of boryl groups in the *ortho*-positions of the complex as in **3** caused the shortening of the axial Fe−N bond lengths (up to 0.02 Å) vs the analogous Fe(II) complex with *ortho*-methyl groups [{*o*-Me-Ph-N=C(Me)-Py-C(Me)=N-Ph-*o*-Me}FeCl$_2$], **1**. The comparisons of the axial bond lengths in *ortho*-boryl-substituted isomer **19** with *para*-boryl-substituted **22** revealed that these bonds are shorter in the *ortho*-isomer (2.201(11) Å) than in the *para*-isomer (2.232(2) Å). An interesting structural feature of **3** is that it exists in the unexpected "up−up" conformer in the solid state, despite reasonable bulkiness of dioxaboranyl substituents in *ortho*-positions. Complexes **21**–**23** afforded very productive catalysts for the production of α-olefins with a more linear Schultz−Flory distribution and with the least amounts of the heavier insoluble fractions of α-olefins than the parent methyl-substituted Fe(II) complex **1**.

Introduction

Fe^{II} catalysts with tridentate bis(imino)pyridine ligands were reported to make α-olefin oligomers with perfect Schultz−Flory distributions, exceptional purities (97–99%), and high productivities.[1b] The results exceed the values reported for catalysts used in the current commercial processes, including the original Ziegler process and Shell's SHOP technology.[2] The presence of sterically small substituents in the *ortho*-positions of the imino aryl group, such as only one methyl group in the *ortho*-positions in complex **1** or the fluorides in the *ortho*-positions in complex **2** groups (Scheme 1), are crucial catalyst structural features needed to produce α-olefins instead of polyethylene.[1,3]

The Fe^{II} complex **1**, with a tridentate bis(imino)pyridine ligand, bearing only one methyl group in the *ortho*-positions of the imino aryl group, was initially determined to be the best for the α-olefin production.[1c,e] However, thorough analysis of complex **1** as a precatalyst for α-olefin oligomerization at the commercially desirable temperature of 120 °C revealed some important shortcomings. Complex **1** is extremely productive, but the lifetime of the catalyst is about 3 min at 120 °C. The resulting exothermic effect is difficult to control. Also, the Schultz−Flory distribution is not linear. The distribution was curved with the light α-olefin fractions (C-4 and C-6) and heavier fractions (C-14 and up) above the theoretical numbers. These shortcomings for the industrial production needed to be addressed through catalyst modifications.

Scheme 1

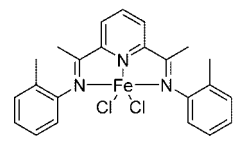

1

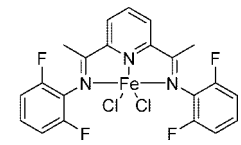

2

In this study, we report Fe^{II} complexes with tridentate bis(imino)pyridine ligands functionalized by boryl substituents, which afford high-temperature catalysts for the production of α-olefins. The four patterns of substitutions were envisioned to make the complexes to produce α-olefins. Pattern **A** has two *ortho*-boryl groups symmetrically placed in two aryl imino groups. The nonsymmetrical patterns[4] **B**, **C**, and **D** have two *ortho*-methyls in one imino aryl group and one boryl group placed in *ortho*-, *meta*-, and *para*-positions correspondingly (Scheme 2).

Results and Discussion

Synthesis. Complex **3** of type **A** was prepared by the following sequence. The condensation reaction between commercially available 1-(6-acetylpyridin-2-yl)ethanone (**4**) and 2-(4,4,5,5-tetramethyl[1,3,2]dioxaborolan-2-yl)phenyl-

[†] This is DuPont contribution #8695.

* Corresponding author. E-mail: alex.s.ionkin@usa.dupont.com.

10.1021/om800036b CCC: $40.75
Publication on Web 03/20/2008

Scheme 2

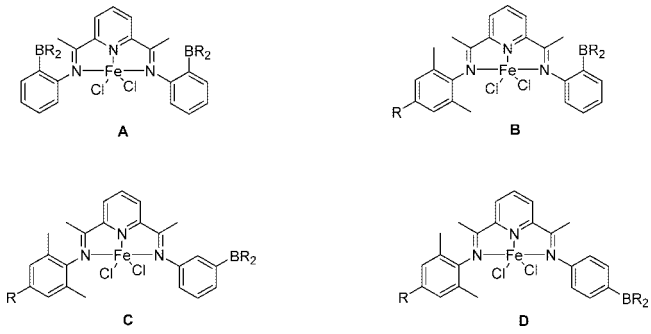

Scheme 3

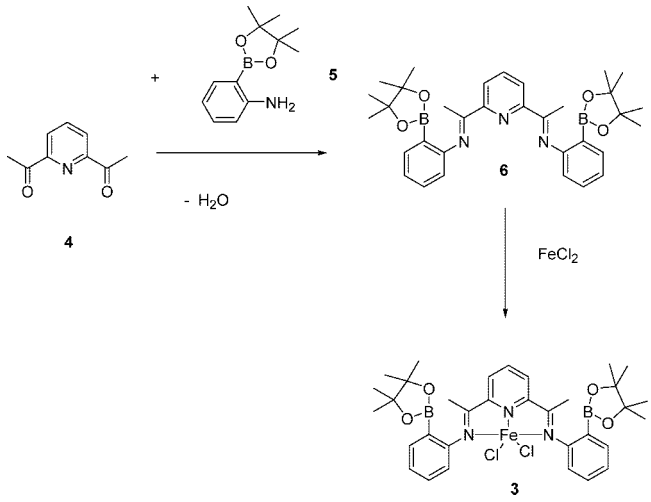

amine (**5**) led to symmetrical bis(imino)pyridine (**6**), with two boryl groups in the *ortho*-positions of the aryl imino arms. The reaction between iron(II) chloride and ligand **6** led to complex **3** of type **A** (Scheme 3).

The structure of complex **3** was determined by X-ray analysis. A crystal of **3** suitable for X-ray analysis was grown from acetonitrile (Figure 1).

Nonsymmetrical complexes of types **B**, **C**, and **D** were prepared by the following methods. Two sets of selective condensations were used to prepare ligands of types **B**, **C**, and **D**. The first condensation reactions between commercially available 1-(6-acetylpyridin-2-yl)ethanone (**4**) and mesitylaniline

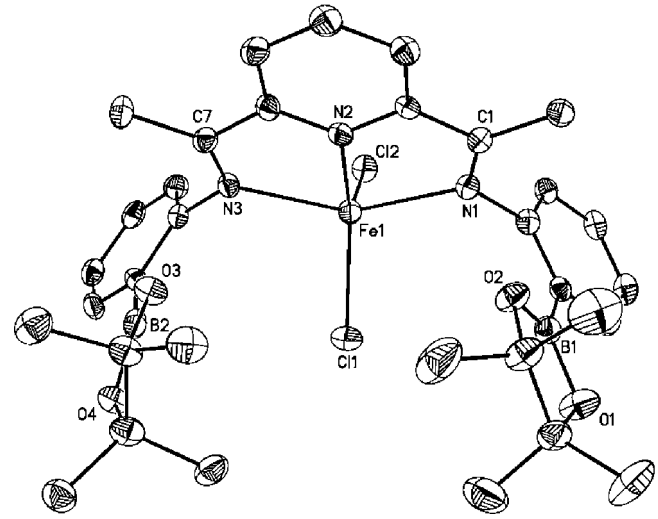

Figure 1. ORTEP drawing of 2,6-bis[1-(2-(4,4,5,5-tetramethyl-[1,3,2]dioxaborolan-2-yl)phenylimino)ethyl]pyridineiron(II) chloride (**3**). The crystal structure is drawn to the 50% probability level. This is an "up−up" conformer.

(**7**) and 4-bromo-2,6-dimethylphenylaniline (**8**) led to nonsymmetrical (imino)(keto)pyridines **9** and **10** respectively (Scheme 4).

The second set of selective condensations between precursors **9** and **10** from one side and borylated anilines **5**, **13**, and **16** from the other side led to the formation of the target ligands of type **B** (**11** and **12**), type **C** (**14**), and type **D** (**17** and **18**). Reactions between the above ligands and iron(II) chloride in THF afforded the final complexes of types **B**−**D** (Scheme 5).

The structures of the nonsymmetrical complexes **19**, **21**, **22**, and **23** were determined by X-ray analysis. Their ORTEP drawings are shown in Figures 2, 3, 4, and 5, respectively.

Solid State Structures of Fe Precatalysts. The complexes **3**, **19**, **22**, and **23** have distorted bipyramidal geometry, which is typical for iron(II) complexes with tridentate bis(imino)pyridine ligands with a ratio of 1:1.[5] The planes of the aryl-substituted arylimino groups of complex **3**, **19**, and **22** are oriented orthogonally to the plane formed by iron and the three nitrogen atoms. The *meta*-boryl-substituted arylimino groups in **21** deviated mostly in this series from the orthogonality. The angles between the mean planes of the nitrogens and iron vs the *meta*-boryl-substituted phenyl rings are 65.7° and 67.4°. The corresponding angles of the mesitylimino arm are 94.4° and 94.5°, which are essentially orthogonal. There are two sets of angles for **21** because the crystal unit cell of complex **21** contains two independent molecules.

(1) For initial publications see (a): Bennett, A. M. A. (DuPont) PCT Int. Appl. WO9827124 A1, 1998, 68 pp. (b) Britovsek, G. J. P.; Gibson, V. C.; Kimberley, B. S.; Maddox, P. J.; McTavish, S. J.; Solan, G. A.; White, A. J. P.; Williams, D. J. *Chem. Commun.* **1998**, 849. (c) Small, B. L.; Brookhart, M. *J. Am. Chem. Soc.* **1998**, *120*, 7143. (d) For recent reviews and papers see: Ittel, S. D.; Johnson, L. K.; Brookhart, M. *Chem. Rev.* **2000**, *100*, 1169. (e) Britovsek, G. J. P.; Gibson, V. C.; Wass, D. F. *Angew. Chem., Int. Ed.* **1999**, *38*, 428. (f) Mecking, S. *Coord. Chem. Rev.* **2000**, *203*, 325. (g) Gibson, V. C.; Spitzmesser, S. K. *Chem. Rev.* **2003**, *103*, 283. (h) Britovsek, G. J. P.; Cohen, S. A.; Gibson, V. C.; van Meurs, M. *J. Am. Chem. Soc.* **2004**, *126*, 10701. (i) Barbaro, P.; Bianchini, C.; Giambastiani, G.; Rios, I. G.; Meli, A.; Oberhauser, W.; Segarra, A. M.; Sorace, L.; Toti, A. *Organometallics* **2007**, *26*, 4639. (k) Bart, S. C.; Lobkovsky, E.; Bill, E.; Wieghardt, K.; Chirik, P. J. *Inorg. Chem.* **2007**, *46*, 7055. (l) Abu-Surrah, A. S.; Qaroush, A. K. *Eur. Polym. J.* **2007**, *43*, 2967. (m) Zhang, S.; Vystorop, I.; Tang, Z.; Sun, W.-H. *Organometallics* **2007**, *26*, 2456. (n) Small, B. L.; Rios, R.; Fernandez, E. R.; Carney, M. J. *Organometallics* **2007**, *26*, 1744. (o) McTavish, S.; Britovsek, G. J. P.; Smit, T. M.; Gibson, V. C.; White, A. J. P.; Williams, D. J. *J. Mol. Catal. A: Chem.* **2007**, *261*, 293. (p) Seitz, M.; Milius, W.; Alt, H. G. *J. Mol. Catal. A: Chem.* **2007**, *261*, 246. (q) Kaul, F. A. R.; Puchta, G. T.; Frey, G. D.; Herdtweck, E.; Herrmann, W. A. *Organometallics* **2007**, *26*, 988. (r) Mahdavi, H.; Badiei, A.; Zohuri, G. H.; Rezaee, A.; Jamjah, R.; Ahmadjo, S. *J. Appl. Polym. Sci.* **2007**, *103*, 1517.

(2) Vogt, D. In *Applied Homogeneous Catalysis with Organometallic Compounds*; Cornils, B., Herrmann, W. Eds.; VCH Publishers: 1996; Vol. 1, p 245.

(3) (a) Chen, Y.; Qian, C.; Sun, J. *Organometallics* **2003**, *22*, 1231. (b) Chen, Y.; Chen, R.; Qian, C.; Dong, X.; Sun, J. *Organometallics* **2003**, *22*, 4312. (c) Schmid, M.; Eberhardt, R.; Klinga, M.; Leskela, M.; Rieger, B. *Organometallics* **2001**, *20*, 2321. (d) Moody, L. S.; MacKenzie, P. B.; Killian, C. M.; Lavoie, G. G.; Ponasik, J. A.; Smith, T. W.; Pearson, J. C.; Barrett, A. G. M. U.S. Pat. Appl. 0049135 A1, 2002. (e) Ionkin, A. S. Marshall, W. J. *Organometallics* **2004**, *23*, 3276. (f) Alt, H. G.; Licht, E. H.; Licht, A. I.; Schneider, K. *J. Coord. Chem. Rev* **2006**, *250*, 2.

(4) (a) Small, B. L.; Brookhart, M. *Macromolecules* **1999**, *32*, 2120. (b) De Boer, E.; Johannes, M.; Deuling, H. H.; Van Der Heijden, H.; Meijboom, N.; Van Oort, A. B.; Van Zon, A. , PCT Int. Appl. WO 2001058874 A1, 2001.

(5) Britovsek, G. J. P.; England, J.; Spitzmesser, S. K.; White, A. J. P.; Williams, D. J. *Dalton Trans.* **2005**, *5*, 945.

Scheme 4. Synthesis of Ligands 11, 12 (Type B); 14 (Type C); and 17, 18 (Type D)

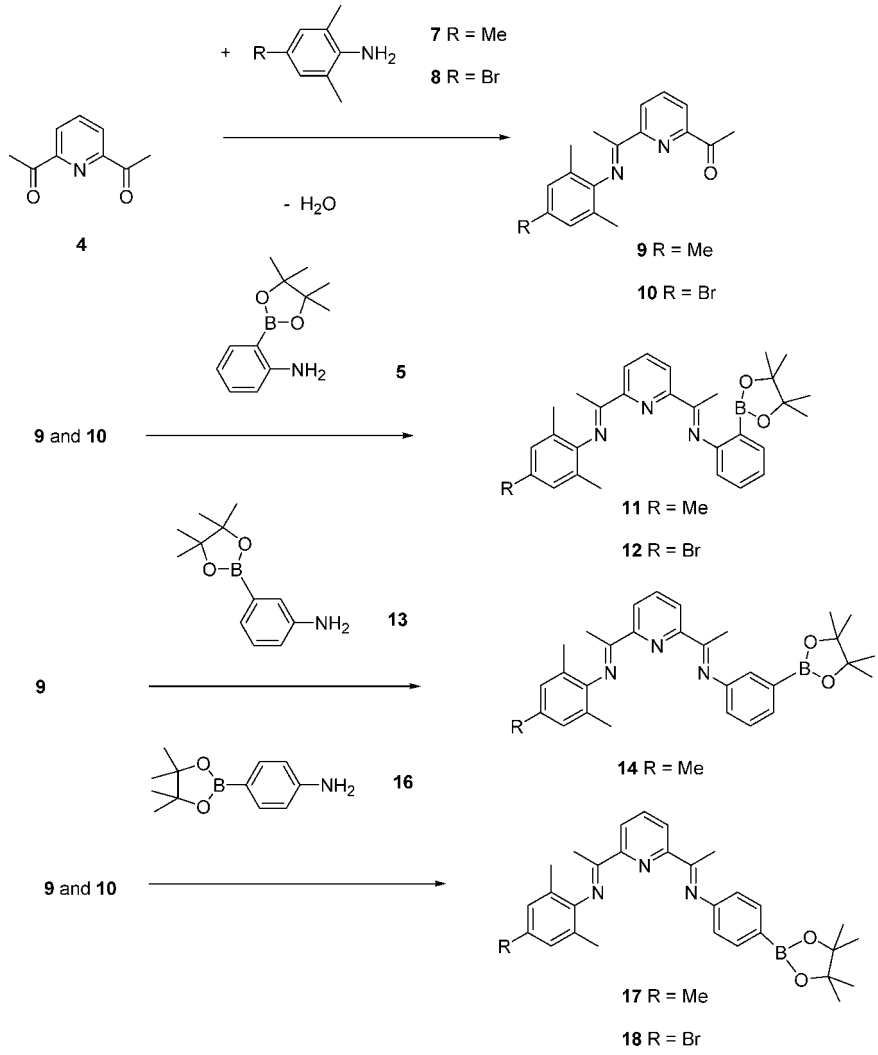

Scheme 5. Iron(II) Tridentate Bis(imino)pyridine Complexes of Types B−D

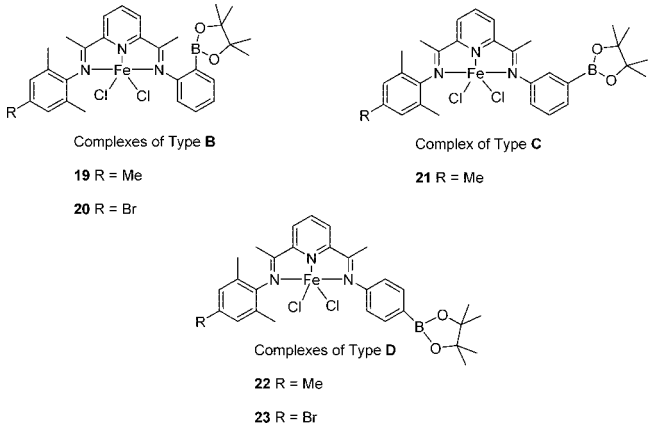

Both boron atoms in **3** remain three-coordinate. There are no short contacts between chloride and boron atoms in complex **3**, which could have resulted in four-coordinated boron atoms. An interesting structural feature of **3** is that it exists as an "up−up" conformer in the solid state despite reasonable bulkiness of the dioxaboranyl substituents in *ortho*-positions.[6] Selected bond lengths of **3** are presented in Table 1.

The axial Fe−N bonds in **3** are actually shorter by an average of 0.015 Å than the corresponding bonds in the methyl-substituted analogue **1**. This bond shortening can be explained by enhanced pπ−dπ back-bonding interactions between iron and the π-accepting boryl-substituted ligand[7] (dioxaboranyl groups are almost coplanar with phenylimino groups, to which they are attached) and by the more σ-donating properties of the boryl-substituted ligand[8] compared with the alkyl-substituted ligand in **1**. It is next to impossible to separate impacts of the

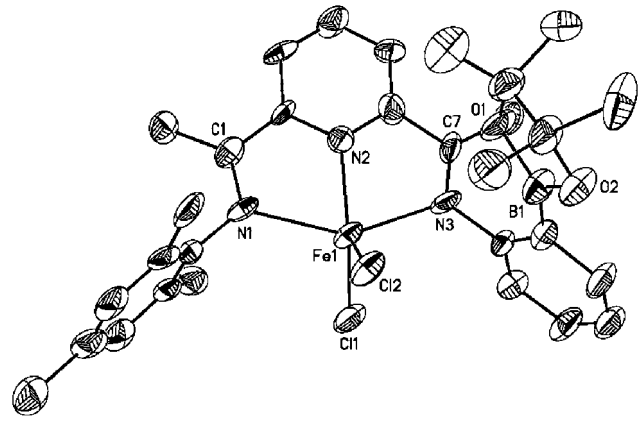

Figure 2. ORTEP drawing of [1-(6-{1-[2-(4,4,5,5-tetramethyl-[1,3,2]dioxaborolan-2-yl)phenylimino]ethyl}pyridin-2-yl)ethylidene](2,4,6-trimethylphenyl)amineiron(II) chloride (**19**). The crystal structure is drawn to the 50% probability level.

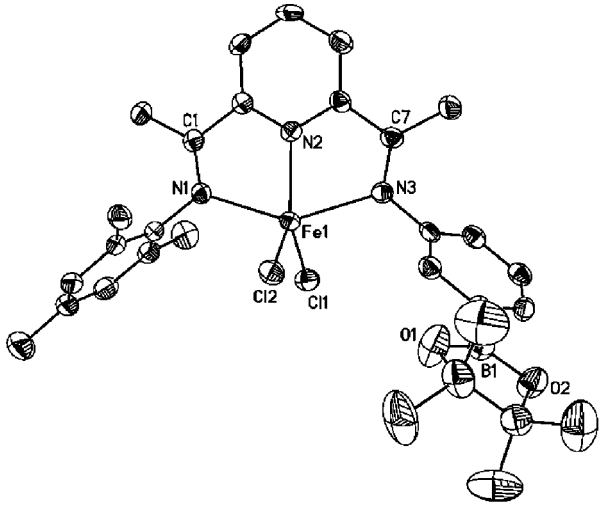

Figure 3. ORTEP drawing of [1-(6-{1-[3-(4,4,5,5-tetramethyl-[1,3,2]dioxaborolan-2-yl)phenylimino]ethyl}pyridin-2-yl)ethylidene](2,4,6-trimethylphenyl)amineiron(II) chloride (**21**). The crystal structure is drawn to the 50% probability level.

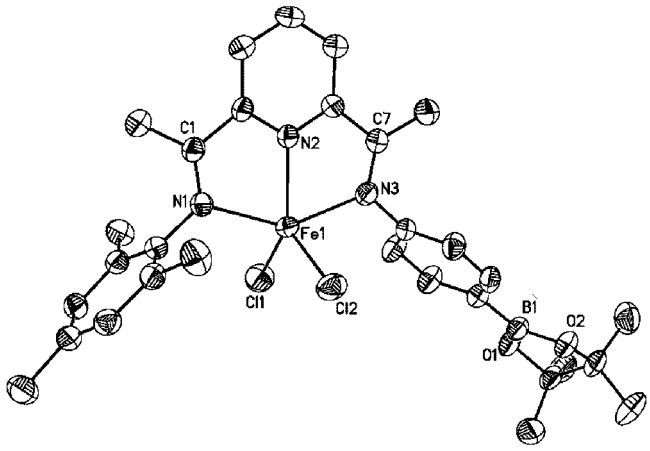

Figure 4. ORTEP drawing of [1-(6-{1-[4-(4,4,5,5-tetramethyl-[1,3,2]dioxaborolan-2-yl)phenylimino]ethyl}pyridin-2-yl)ethylidene](2,4,6-trimethylphenyl)amineiron(II) chloride (**22**). The crystal structure is drawn to the 50% probability level.

above interactions, but the more electron-donating properties of the boryl-substituted ligand seem to be the cause of the shortening. The comparison of bond lengths of the imino groups in **3** and **1** shows the reverse trends. The C═N bonds in **3** are longer than in **1** by 0.01 Å. It may be an indication that Fe−N bonds in **3** are stronger than in **1**. The C═N bonds get longer with the shortening of Fe−N bonds in X-ray-analyzed Fe^{II} complexes with tridentate bis(imino)pyridine ligands.[9]

The axial Fe−N bonds from the mesityl imino arm in **22** (2.247(2) Å) is longer than those from the borylated imino arm (2.232(2) Å for **22**). This elongation of the Fe−N bonds from the mesityl side is due to steric repulsion of the two *ortho*-methyl groups and the iron core of the molecules. The boron atoms in **19** and **22** remain tricoordinated and do not have short contacts with chlorides or any other atoms. The rest of the structural data are in agreement with the previous structural studies of iron(II) complexes with tridentate bis(imino)pyridine ligands.

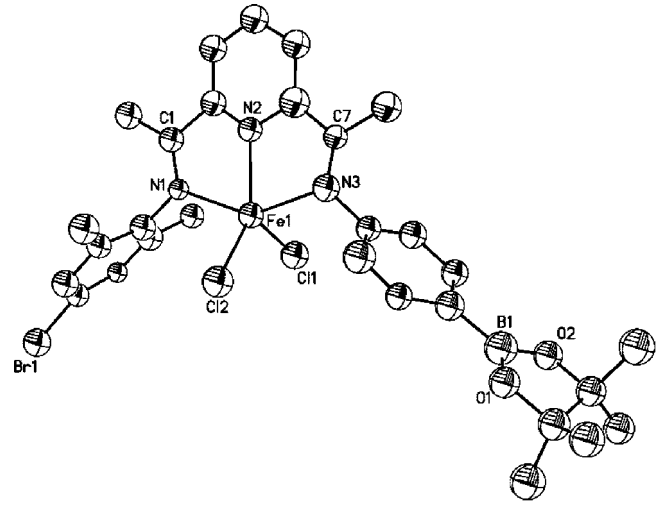

Figure 5. ORTEP drawing of (4-bromo-2,6-dimethylphenyl)[1-(6-{1-[4-(4,4,5,5-tetramethyl[1,3,2]dioxaborolan-2-yl)phenylimino]-ethyl}pyridin-2-yl)ethylidene]amineiron(II) chloride (**23**). The crystal structure is drawn to the 50% probability level.

The complexes **19** and **23** were analyzed by X-ray, however, due to the small crystallite size; the overall structure quality is poor and only serves to establish the connectivity for this study. The correlations of the bond lengths in **19** and **23** with other structures are not discussed for that reason here.

Oligomerization of Ethylene to α-Olefins by Fe(II) Dichloride Complexes 19, 20, 21, 22, and 23. Ethylene oligomerizations were done using the equipment and procedure described in the Experimental Section. The purpose was to evaluate the catalysts for the production of α-olefins. Catalyst lifetimes, productivities, temperature stability, and product distributions were of greatest interest. The performances of the nonsymmetrical boryl-containing precatalysts are compared to that of the standard symmetric *ortho*-methyl candidate, **1**.

A catalyst lifetime was defined as the time from introduction of ethylene to the reactor until its uptake was no longer detected by the mass flow sensor. Since the catalysts have wide ranging activities (speeds) and temperature sensitivities, the amounts of precatalysts injected were adjusted until exothermic effects of no greater than 2 °C were achieved and until similar amounts of olefins were made for all precatalysts. The former ensured that the lifetimes were not affected by catalysts being exposed to temperatures more than 2 °C higher than the intended setpoint. The latter was desired to make sure the data were not affected by nonlinearities in the analytical methods.

Figure 6 is a plot of ethylene uptakes for several catalysts. There is an initial rapid consumption of ethylene followed by a tailing-off. The noise and larger perturbations in the tail sections of the curves are a result of using a single ethylene feed orifice to cover the large uptake range. The larger

(6) (a) Tellmann, K. P.; Gibson, V. C.; White, A. J. P.; Williams, D. J. *Organometallics* **2005**, *24*, 280. (b) Ionkin, A. S.; Marshall, W. J.; Adelman, D. J.; Bobik Fones, B.; Fish, B. M.; Schiffhauer, M. F. *Organometallics* **2006**, *25*, 2978.

(7) (a) Sakaki, S.; Biswas, B.; Musashi, Y.; Sugimoto, M. *J. Organomet. Chem.* **2000**, *611*, 288. (b) Wrackmeyer, B.; Tok, O. L.; Ayazi, A.; Maisel, H. E.; Herberhold, M. *Magn. Reson. Chem.* **2004**, *42*, 827. (c) Exner, O.; Bose, R. *Collect. Czech. Chem. Commun.* **1974**, *39*, 2234. (d) Sakaki, S.; Kai, S.; Sugimoto, M. *Organometallics* **1999**, *18*, 4825.

(8) (a) Wrackmeyer, B.; Kerschl, S.; Klaus, U. *Z. Naturforsch., B: Chem. Sci.* **2002**, *57*, 1251. (b) Sugihara, Y.; Takakura, K.; Murafuji, T.; Miyatake, R.; Nakasuji, K.; Kato, M.; Yano, S. *J. Org. Chem.* **1996**, *61*, 6829.

(9) (a) Britovsek, G. J. P.; Mastroianni, S.; Solan, G. A.; Baugh, S. P. D.; Redshaw, C.; Gibson, V. C.; White, A. J. P.; Williams, D. J.; Elsegood, M. R. J. *Chem.−Eur. J.* **2000**, *6*, 2221. (b) Bianchini, C.; Mantovani, G.; Meli, A.; Migliacci, F.; Zanobini, F.; Laschi, F.; Sommazzi, A. *Eur. J. Inorg. Chem.* **2003**, *8*, 1620.

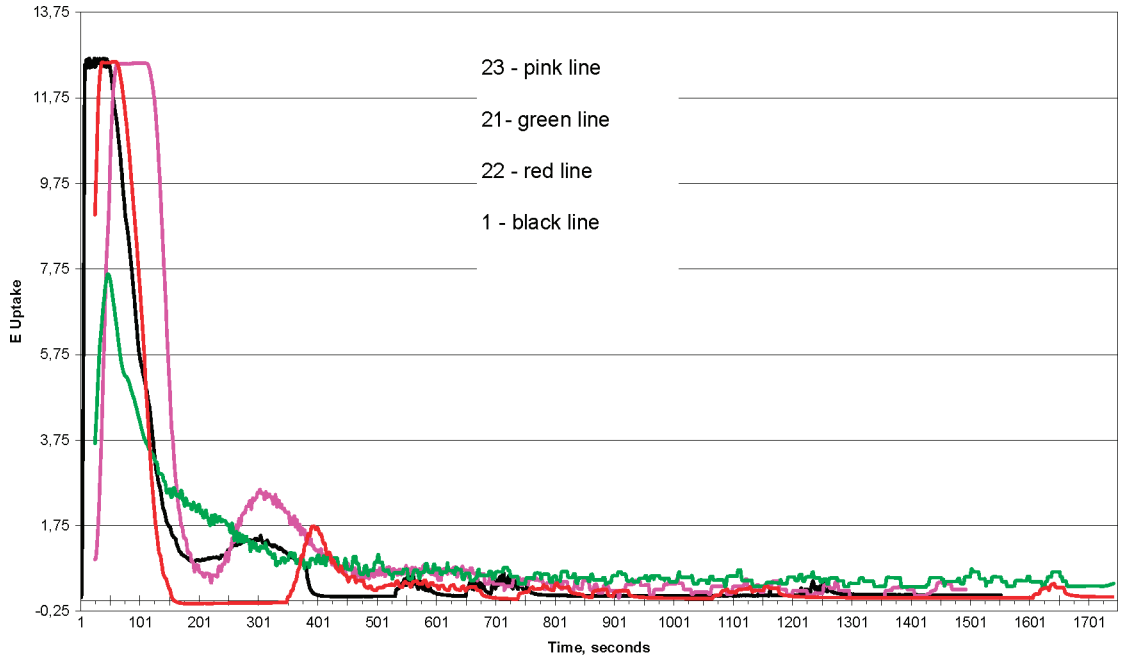

Figure 6. Graph of ethylene uptake of complexes **1**, **21**, **22**, and **23** in catalytic oligomerization of ethylene at 120 °C.

Table 1. Selected Bond Lengths (Å) for 1, 3, 19, 21, and 23

	1	**3**	**19**	**21**	**22**	**23**
axial (imino) N−Fe bond	2.2303(16) Fe−N1	2.220(4) Fe−N1	2.225(10) Fe−N1 mesityl side	2.259(3) Fe−N1 mesityl side	2.247(2) Fe−N1 mesityl side	2.220(11) Fe−N1 4-bromo-2,6-dimethylphenyl side
axial (imino) N−Fe bond	2.2424(17) Fe−N3	2.222(4) Fe−N3	2.201(11) Fe−N3 boryl side	2.272(3) Fe−N3 boryl side	2.232(2) Fe−N3 boryl side	2.234(13) Fe−N3 boryl side
basel (central) N−Fe bond	2.0943(16) Fe−N2	2.113(4) Fe−N2	2.130(10) Fe−N2	2.107(3) Fe−N2	2.121(2) Fe−N2	2.103(12) Fe−N2
C═N	1.281(2) N1−C1	1.290(5) N1−C1	1.288(14) N1−C1 mesityl side	1.272(4) N1−C1 mesityl side	1.285(3) N1−C1 mesityl side	1.289(16) N1−C1 4-bromo-2,6-dimethylphenyl side
C═N	1.287(3) N3−C7	1.272(5) N3−C7	1.261(15) N3−C7 boryl side	1.290(4) N3−C7 boryl side	1.288(3) N3−C7 boryl side	1.242(17) N3−C7 boryl side

Table 2. α-Olefins from Ethylene Oligomerizations by Iron(II) Complexes 1, 19, 20, 21, 22, and 23[a]

entry	precatalyst and amount, μmol	amount cocatalyst, MMAO, mmol	temperature, °C	"*K*" value Schultz−Flory distribution [b]	kg of LAO per g of catalyst	% solids total LAO [c]	SFD R^2
1	**3**, 0.15	2.26	120 and 100		traces		
2	**19**, 0.16	2.26	120	0.79	71	57.94	N/A
3	**19**, 0.08	2.26	100	0.77	219	70.63	N/A
4	**20**, 0.15	2.26	120 and 100		traces		
5	**21**, 0.16	2.26	120	0.66	122	4.00	0.9971
6	**21**, 0.08	2.26	100	0.68	178	3.87	0.9902
7	**22**, 0.16	2.26	120	0.64	168	3.01	0.9979
8	**22**, 0.08	2.26	100	0.67	855	3.54	0.9989
9	**23**, 0.15	2.26	120	0.63	266	1.13	0.9978
10	**23**, 0.07	2.26	100	0.65	752	2.53	0.9992
11	**1**, 0.062	1.13	120	0.59	458	3.44	0.9862

[a] Conditions: solvent, *o*-xylene, 600 mL; pressure, 700 psig. [b] Determined from GC, using extrapolated values for C-10 and C-12. [c] Xylenes insoluble fraction of α-olefins.

disturbances are caused by the orifice opening slightly in response to a small autoclave pressure drop. Considering the individual traces in Figure 6, it appears that the boryl-containing catalysts, **21**–**23**, showed more activity beyond 800 s than did the *ortho*-methyl, **1**. This suggests the boryl group extended the lifetime relative to that of the standard catalyst.

Results used to evaluate productivities, temperature stability, and product distributions of the precatalysts are shown in Table 2. Complexes with *ortho*-borylated moieties, such as bis-borylated complex **3** and nonsymmetrical monoborylated complex **20**, were found to have very low activities in α-olefin oligomerization experiments within the tested range of temperatures (60–130 °C). The nonsymmetrical monoborylated complex **19** behaved as a polymerization catalyst at high temperatures to some degree because it produced a lot of solids (Table 3, seventh column). The formation of up to 70% solids may be an indication of the disproportionation of the catalyst **19** to symmetrical tetra-*ortho*-methyl-substituted derivative **24** at this

Table 3. Summary of Crystal Data, Data Collection, and Structural Refinement Parameters for 1, 3, and 19

	1	3	19
empirical formula	$C_{24}H_{25}Cl_4FeN_3$	$C_{37}H_{47}B_2Cl_2FeN_5O_4$	$C_{36}H_{42}BCl_2FeN_3O_2$
fw	553.12	774.17	686.29
cryst color, form	blue, needle	blue, rec. plate	blue, needle
cryst syst	monoclinic	monoclinic	monoclinic
space group	*P*2(1)/*c*	*P*2(1)/*n*	*P*2(1)/*c*
a (Å)	10.4140(5)	12.6115(19)	8.65(2)
b (Å)	15.2465(8)	16.284(2)	23.25(6)
c (Å)	15.8488(8)	19.867(3)	17.26(4)
α (deg)	90	90	90
β (deg)	92.3650(10)	104.933(3)	90.99(4)
γ (deg)	90	90	90
V (Å^3)	2514.3(2)	3942.1(10)	3471(14)
Z	4	4	4
density (g/cm^3)	1.461	1.304	1.313
abs *μ* (mm^{-1})	1.042	0.562	0.624
F(000)	1136	1624	1440
cryst size (mm)	0.32 × 0.06 × 0.02	0.34 × 0.25 × 0.03	0.45 × 0.08 × 0.01
temp (°C)	−100	−100	−100
scan mode	*ω*	*ω*	*ω*
detector	Bruker-CCD	Bruker-CCD	Bruker-CCD
θ_{max} (deg)	27.96	27.12	25.98
no. obsrvd reflns	37 670	29 039	17 417
no. uniq reflns	6038	8687	6644
R_{merge}	0.055	0.147	0.390
no. params	358	446	449
S^b	1.02	0.869	0.869
R indices [$I > 2\sigma(I)$]^a	wR2 = 0.075, R1 = 0.036	wR2 = 0.126, R1 = 0.068	wR2 = 0.223, R1 = 0.114
R indices (all data)^a	wR2 = 0.084, R1 = 0.060	wR2 = 0.162, R1 = 0.173	wR2 = 0.367, R1 = 0.386
max diff peak, hole (e/Å^3)	0.288, −0.325	0.364, −0.342	0.703, −0.868

^{a} $R1 = \sum|F_o - F_c|/\sum F_o$, $wR2 = \{\sum[w(F_o^2 - F_c^2)^2]/\sum[w(F_o^2)^2]\}^{1/2}$ (sometimes denoted as wR_2). ^{b} $GooF = S = \{\sum[w(F_o^2 - F_c^2)^2]/(n - p)\}^{1/2}$, where *n* is the number of reflections and *p* is the total number of refined parameters.

Scheme 6

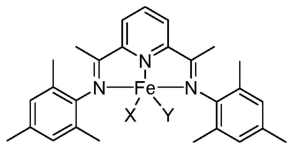

24

high temperature, which is known to result in polymer formation.[1,10]

Precatalysts **21**–**23**, which have *meta*- or *para*-boryl imino arm groups, show high activities. Comparisons of productivities at 120 °C of the latter group to that of **1** indicate that **1** is nearly 2 times more productive than any of the boryl-containing catalysts. While this may seem like a disadvantage, the amount of precatalyst needed, even for the boryl-containing complexes, adds insignificant expense to the cost of making α-olefins because they are so active.

An indication of the temperature sensitivity of a catalyst can be achieved by comparing its productivities at 100 and 120 °C. Precatalyst **21** has nearly the same productivity at both temperatures, whereas **22** and **23** are greatly different. This suggests that **21** is much more thermally stable than are **22** and **23**. Support for this is seen in Figure 6. The ethylene uptake profiles show that **21** continued to consume ethylene most steadily to near the end of the experiment.

The temperature stability and productivities have implications for α-olefin reactor design. For example, in a plug flow design, an unstable but highly productive catalyst will require more frequent injections of less catalyst than will a stable, less active catalyst. While a less active but more stable catalyst will need to be injected at a higher rate, fewer injection points will be needed. Also, a more stable catalyst will facilitate operation at a higher temperature. This keeps the higher molecular weight oligomers in solution to delay equipment fouling.

Of particular importance is the molecular weight distribution of products made by a catalyst. The best that can be expected is for the products to fit an ideal Schultz−Flory distribution.[11] A single factor used to characterize this distribution is the Schultz−Flory *K* value. It is defined as

$$K = n(C_{n+2}\ \text{olefin})/n(C_n\ \text{olefin})$$

wherein $n(C_n$ olefin) is the number of moles of olefin containing *n* carbon atoms, and $n(C_{n+2}$ olefin) is the number of moles of olefin containing $n+2$ carbon atoms, or in other words the next higher oligomer of C_n olefin. From this, the weight fractions of the various olefins in the resulting oligomeric reaction product mixture can be determined. The *K* factor is usually preferred to be in the range of about 0.6 to about 0.8 to make the α-olefins of the most commercial interest. It is also desirable to be able to vary this factor so as to make a range of products. As seen in Table 2, small changes can be achieved by adjusting the temperature.

Excluding the *K* values for **19**, evaluation of the data in Table 2 indicates that precatalyst **21**, with a *meta*-boryl group, gave the highest *K* values of 0.68 at 100 °C and 0.66 at 120 °C (entries 5 and 6 in Table 2). The *meta*-boryl group creates more steric bulk around the metal center than *para*-substitution patterns of **22** and **23**. The increase of the steric bulk around iron leads usually to an increase in the *K* value.[9b,12,13a] The drop

(10) Small, B. L.; Brookhart, M.; Bennett, A. M. A. *J. Am. Chem. Soc.* **1998**, *120*, 4049.

(11) Elvers, B., et al., Ed. *Ullmann's Encyclopedia of Industrial Chemistry*; VCH Verlagsgesellschaft mbH: Weinheim, 1989; Vol. A13, pp 243–247 and 275–276..

(12) Britovsek, G. J. P.; Gibson, V. C.; Mastroianni, S.; Oakes, D. C. H.; Redshaw, C.; Solan, G. A.; White, A. J. P.; Williams, D. J. *Eur. J. Inorg. Chem.* **2001**, *2*, 431.

Table 4. Summary of Crystal Data, Data Collection, and Structural Refinement Parameters for 21, 22, and 23

	21	22	23
empirical formula	$C_{61}H_{74}B_2Cl_6Fe_2N_6O_4$	$C_{30}H_{36}BCl_2FeN_3O_2$	$C_{29}H_{33}BBrCl_2FeN_3O_2$
fw	1301.28	608.18	673.05
cryst color, form	blue, rect plate	blue, prism	blue, needle
cryst syst	monoclinic	monoclinic	monoclinic
space group	*P*2(1)/*c*	*P*2(1)/*c*	*P*2(1)
a (Å)	31.466(3)	14.116(4)	14.112(14)
b (Å)	8.8961(9)	15.902(5)	15.854(17)
c (Å)	25.037(3)	14.105(4)	13.830(15)
α (deg)	90	90	90
β (deg)	111.985(2)	101.311(5)	100.75(2)
γ (deg)	90	90	90
V (Å^3)	6498.8(12)	3104.7(16)	3040(6)
Z	4	4	4
density (g/cm^3)	1.33	1.301	1.471
abs *μ* (mm^{-1})	0.742	0.688	2.017
F(000)	2712	1272	1376
cryst size (mm)	0.50 × 0.18 × 0.06	0.50 × 0.24 × 0.15	0.12 × 0.04 × 0.01
temp (°C)	−100	−100	−100
scan mode	*ω*	*ω*	*ω*
detector	Bruker-CCD	Bruker-CCD	Bruker-CCD
θ_{max} (deg)	28.27	28.51	26.99
no. obsrvd reflns	52 486	25 834	22 463
no. uniq reflns	16 031	7769	6457
R_{merge}	0.105	0.084	0.705
no. params	748	361	355
S [b]	0.987	0.999	0.684
R indices [$I > 2\sigma(I)$][a]	wR2 = 0.116, R1 = 0.058	wR2 = 0.125, R1 = 0.052	wR2 = 0.206, R1 = 0.092
R indices (all data)[a]	wR2 = 0.144, R1 = 0.144	wR2 = 0.149, R1 = 0.099	wR2 = 0.350, R1 = 0.366
max diff peak, hole (e/Å^3)	0.690, −0.909	0.659, −0.793	0.859, −1.231

[a] $R1 = \sum|F_o - F_c|/\sum F_o$, $wR2 = \{\sum[w(F_o^2 - F_c^2)^2]/\sum[w(F_o^2)^2]\}^{1/2}$ (sometimes denoted as wR_2). [b] $GooF = S = \{\sum[w(F_o^2 - F_c^2)^2]/(n - p)\}^{1/2}$, where *n* is the number of reflections and *p* is the total number of refined parameters.

in *K* values by 0.02 upon increasing the temperature from 100 to 120 °C is normal dependency for the Versipol family of catalysts.[1] Precatalysts **22** and **23** have both *para*-boryl groups in one imino arm and differ only by the *para*-substituent in another imino arm (methyl in **22** and bromo in **23**). The methyl derivative **22** gave a set of *K* values of 0.64 and 0.67, which are higher than 0.63 and 0.65 for the bromo derivative **23** at the same two temperatures. Both sets of *K* values are quite acceptable for commercial application. The parent catalyst from complex **1**, with two *ortho*-methyl groups on both imino arms, gave α-olefins with a *K* value below 0.6.

In Table 2 is a column labeled "% solids of total LAO". That represents the weight percent of α-olefin made that was not soluble in *o*-xylene at room temperature. Since these have very limited commercial value, they represent an ethylene yield loss and so should be minimized. The values for precatalyst **23** were the lowest, with only 1.13 and 2.53 wt % at 120 and 100 °C, respectively (entries 9 and 10 in Table 2).

The goodness-of-fit of the product distribution to the ideal Schultz−Flory distribution was mentioned earlier as a measure of the desirability of a catalyst. Using a form of the Schultz−Flory equation given in previous work,[13] a plot of the degree of polymerization (D_p) minus 2 vs the logarithm of the quantity the weight fraction with a certain degree of polymerization (M_{Dp}) divided by that degree of polymerization is made to judge the fit to the ideal distribution. Figure 7 shows the results for precatalysts **21**–**23** and **1**. Straight lines are drawn through all of the sets of data. It is clear that the data points for precatalyst **1** deviate more from its line on the high and low D_p ends of the plot. This is supported by the higher correlation coefficients (SFD R^2) seen for the borylated precatalysts seen in Table 2 or in Figure 7. The superior linearity of precatalysts **21**−**23** is explained by the nonsymmetrical nature of the ligand.[4]

In conclusion, the Fe-based bis(imino)pyridine complexes **21**−**23** functionalized nonsymmetrically by the boryl groups are more thermally stable but less productive than is the symmetric parent complex **1**. Additionally, they make more desirable product distributions that are more ideal. Precatalyst **23** has the added advantage that it makes considerably less solids than precatalyst **1**.

Experimental Section

All air-sensitive compounds were prepared and handled under a N_2/Ar atmosphere using standard Schlenk and inert-atmosphere box techniques. Anhydrous solvents were used in the reactions. Solvents were distilled from drying agents or passed through columns under an argon or nitrogen atmosphere. Anhydrous iron(II) chloride, 1-(6-acetylpyridin-2-yl)ethanone, 2-(4,4,5,5-tetramethyl[1,3,2]dioxaborolan-2-yl)phenylamine, 4-(4,4,5,5-tetramethyl[1,3,2]dioxaborolan-2-yl)phenylamine, 3-(4,4,5,5-tetramethyl[1,3,2]dioxaborolan-2-yl)-phenylamine, and THF were purchased from Aldrich. Complex **1** was prepared according to the literature.[1,10]

2,6-Bis[1-(2-(4,4,5,5-tetramethyl[1,3,2]dioxaborolan-2-yl)-phenylimino)ethyl]pyridine (6). A 1.77 g (0.0108 mol) sample of 1-(6-acetylpyridin-2-yl)ethanone (**4**), 5.0 g (0.0228 mol) of 2-(4,4,5,5-tetramethyl[1,3,2]dioxaborolan-2-yl)phenylamine (**5**), 100 mL of toluene, and 100 g of the fresh molecular sieves were kept at 100 °C for 3 days. The molecular sieves were removed by filtration. The solvent was removed in a rotary evaporator, and the residue was recrystallized from 20 mL of ethanol. The yield of 2,6-bis[1-(2-(4,4,5,5-tetramethyl[1,3,2]dioxaborolan-2-yl)phenylimino)ethyl]pyridine (**6**) was 4.48 g (73%) as a pale yellow solid. ^{1}H NMR (500 MHz, Tol-D$_8$, TMS): *δ* 0.95 (s, 24H, Me), 2.31 (s, 6H, Me), 6.63 (m, 2H, Arom-H), 6.90 (m, 2H, Arom-H), 7.21 (m, 2H, Arom-H), 7.45 (t, $^3J_{HH}$ = 7.8 Hz, 1H, Py-H), 8.05 (m, 2H, Arom-

(13) (a) Ionkin, A. S.; Marshall, W. J.; Adelman, D. J.; Bobik Fones, B.; Fish, B. M.; Schiffhauer, M. F.; Soper, P. D.; Waterland, R. L.; Spence, R. E.; Xie, T. *J. Polym. Sci., Part A: Polym. Chem.* **2008**, *46*, 585. (b) Ionkin, A. S.; Marshall, W. J.; Adelman, D. J.; Shoe, A. L.; Spence, R. E.; Xie, T. *J. Polym. Sci., Part A: Polym. Chem.* **2006**, *44*, 2615.

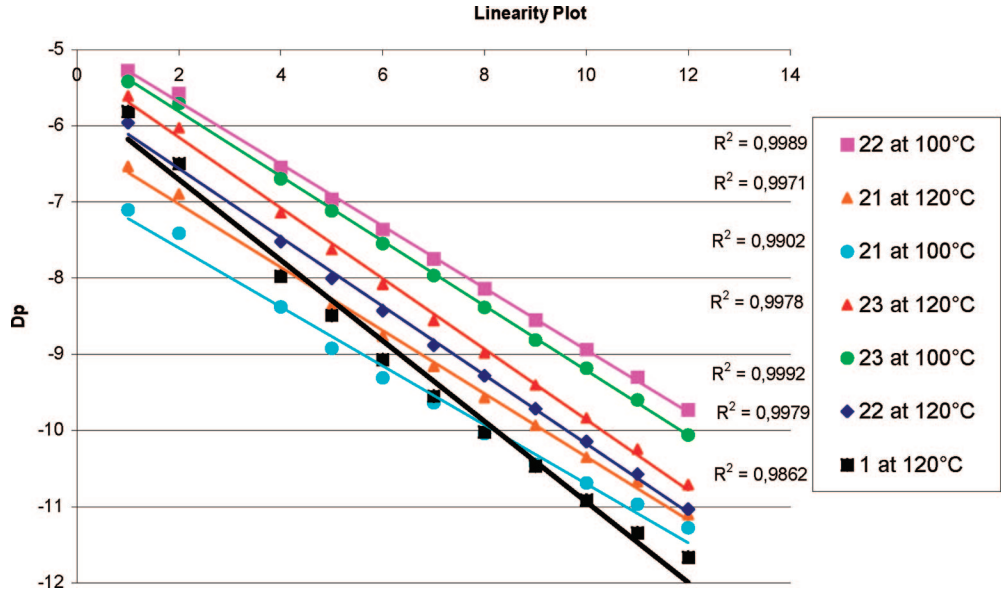

Figure 7. Distribution of α-olefins from C-2 to C-14 for precatalysts **1**, **21**, **22**, and **23**.

H), 8.50 (d, $^3J_{HH}$ = 7.8 Hz, 2H, Py-H). ^{13}C NMR (500 MHz, Tol-D_8, (selected signals)): δ 165.8 (C═N). Anal. Calcd for $C_{33}H_{41}B_2N_3O_4$ (MW: 565.32): C, 70.11; H, 7.31; N, 7.43. Found: C, 70.29; H, 7.33; N, 7.64.

2,6-Bis[1-(2-(4,4,5,5-tetramethyl[1,3,2]dioxaborolan-2-yl)-phenylimino)ethyl]pyridineiron(II) Chloride (3). A 1.31 g (0.0023 mol) sample of 2,6-bis[1-(2-(4,4,5,5-tetramethyl[1,3,2]dioxaborolan-2-yl)phenylimino)ethyl]pyridine (**6**) was dissolved in 40 mL of THF. Iron(II) chloride (0.26 g, 0.0021 mol) was added in the reaction mixture in one portion. The resultant blue precipitate was filtered after 12 h of stirring, washed twice by 20 mL of pentane, and dried at 1 mm vacuum. Yield of 2,6-bis[1-(2-(4,4,5,5-tetramethyl[1,3,2]dioxaborolan-2-yl)phenylimino)ethyl]pyridineiron(II) chloride (**3**) was 1.31 g (92%). Anal. Calcd for $C_{33}H_{41}B_2Cl_2FeN_3O_4$ (MW: 692.07): C, 57.27; H, 5.97; N, 6.07. Found: C, 57.46; H, 6.09; N, 6.24. The structure was determined by X-ray analysis.

1-{6-[1-(2,4,6-Trimethylphenylimino)ethyl]pyridin-2-yl}ethanone (9). A 20.0 g (0.123 mol) sample of 1-(6-acetylpyridin-2-yl)ethanone (**4**), 14.92 g (0.110 mol) of 2,4,6-trimethylphenylamine (**7**), and 300 mL of *n*-propanol with a few crystals of *p*-toluenesulfonic acid were stirred at room temperature for 36 h in a 500 mL flask under the flow of nitrogen. The resultant yellow precipitate was filtered and washed by 20 mL of methanol. It was then dried at 1 mm vacuum overnight. The yield of 1-{6-[1-(2,4,6-trimethylphenylimino)ethyl]pyridin-2-yl}ethanone (**9**) was 9.01 g (26%) as a yellow solid. ^{1}H NMR (500 MHz, CD_2Cl_2, TMS): δ 1.90 (s, 6H, Me), 2.20 (s, 3H, Me), 2.28 (s, 3H, Me), 2.75 (s, 3H, Me), 6.90 (s, 2H, Arom-H), 7.90 (t, $^3J_{HH}$ = 8.0 Hz, 1H, Py-H), 8.09 (d, $^3J_{HH}$ = 8.0 Hz, 1H, Py-H), 8.55 (d, $^3J_{HH}$ = 8.0 Hz, 1H, Py-H). ^{13}C NMR (500 MHz, CD_2Cl_2, TMS (selected signals)): δ 167.3 (C═N), 200.0 (C═O). Anal. Calcd for $C_{18}H_{20}N_2O$ (MW: 280.36): C, 77.11; H, 7.19; N, 9.99. Found: C, 77.13; H, 7.20; N, 10.20.

1-{6-[1-(4-Bromo-2,6-dimethylphenylimino)ethyl]pyridin-2-yl}ethanone (10). A 22.5 g (0.138 mol) sample of 1-(6-acetylpyridin-2-yl)ethanone (**4**), 25.0 g (0.125 mol) of 4-bromo-2,6-dimethylphenylamine (**8**), and 300 mL of *n*-propanol with a few crystals of *p*-toluenesulfonic acid were stirred at room temperature for 36 h in a 500 mL flask under the flow of nitrogen. The resultant yellow precipitate was filtered and washed by 20 mL of methanol. It was then dried at 1 mm vacuum overnight. The yield of 1-{6-[1-(4-bromo-2,6-dimethylphenylimino)ethyl]pyridin-2-yl}ethanone (**10**) was 19.08 g (44%) as a yellow solid. ^{1}H NMR (500 MHz, CD_2Cl_2, TMS): δ 1.95 (s, 6H, Me), 2.22 (s, 3H, Me), 2.30 (s, 3H, Me), 6.80 (s, 2H, Arom-H), 7.95 (t, $^3J_{HH}$=8.0 Hz, 1H, Py-H), 8.15 (d, $^3J_{HH}$ = 8.0 Hz, 1H, Py-H), 8.40 (d, $^3J_{HH}$ = 8.0 Hz, 1H, Py-H). ^{13}C NMR (500 MHz, CD_2Cl_2, TMS (selected signals)): δ 168.4 (C═N), 199.5 (C═O). Anal. Calcd for $C_{17}H_{17}BrN_2O$ (MW: 345.23): C, 59.14; H, 4.96; N, 8.11. Found: C, 59.18; H, 5.07; N, 8.15.

[1-(6-{1-[2-(4,4,5,5-Tetramethyl[1,3,2]dioxaborolan-2-yl)-phenylimino]ethyl}pyridin-2-yl)ethylidene](2,4,6-trimethylphenyl)amine (11). A 5.0 g (0.0178 mol) sample of 1-{6-[1-(2,4,6-trimethylphenylimino)ethyl]pyridin-2-yl}ethanone (**9**), 5.0 g (0.0228 mol) of 2-(4,4,5,5-tetramethyl[1,3,2]dioxaborolan-2-yl)phenylamine (**5**), 100 mL of toluene, and 100 g of fresh molecular sieves were kept at 100 °C for 3 days. The molecular sieves were removed by filtration. The solvent was removed in a rotary evaporator, and the residue was recrystallized from 10 mL of ethanol. The yield of [1-(6-{1-[2-4,4,5,5-tetramethyl[1,3,2]dioxaborolan-2-yl)phenylimino]ethyl}-pyridin-2-yl)ethylidene](2,4,6-trimethylphenyl)amine (**11**) was 3.91 g (71%) as a pale yellow solid. ^{1}H NMR (500 MHz, Tol-D_8, TMS): δ 1.10 (s, 12H, Me), 2.00 (s, 6H, Me), 2.25 (s, 3 H, Me), 2.30 (s, 3H, Me), 2.45 (s, 3H, Me), 6.40 (m, 1H, Arom-H), 6.60 (m, 1H, Arom-H), 7.00 (m, 1H, Arom-H), 7.20 (m, 1H, Arom-H), 7.50 (t, $^3J_{HH}$ = 8.0 Hz, 1H, Py-H), 7.90 (s, 2H, Arom-H), 8.10 (d, $^3J_{HH}$ = 8.0 Hz, 1H, Py-H), 8.55 (d, $^3J_{HH}$ = 8.0 Hz, 1H, Py-H). ^{13}C NMR (500 MHz, Tol-D_8, (selected signals)): δ 166.17 (C═N), 167.60 (C═N). Anal. Calcd for $C_{30}H_{36}BN_3O_2$ (MW: 481.44): C, 74.84; H, 7.54; N, 8.73. Found: C, 75.05; H, 7.63; N, 8.92.

(4-Bromo-2,6-dimethylphenyl)[1-(6-{1-[2-(4,4,5,5-tetramethyl[1,3,2]dioxaborolan-2-yl)phenylimino]ethyl}pyridin-2-yl)ethylidene]amine (12). A 6.30 g (0.0182 mol) sample of 1-{6-[1-(4-bromo-2,6-dimethylphenylimino)ethyl]pyridin-2-yl}ethanone (**10**), 5.0 g (0.0228 mol) of 2-(4,4,5,5-tetramethyl[1,3,2]dioxaborolan-2-yl)phenylamine (**5**), 100 mL of toluene, and 100 g of fresh molecular sieves were kept at 100 °C for 3 days. The molecular sieves were removed by filtration. The solvent was removed in a rotary evaporator, and the residue was recrystallized from 10 mL of ethanol. The yield of (4-bromo-2,6-dimethylphenyl)[1-(6-{1-[2-(4,4,5,5-tetramethyl[1,3,2]dioxaborolan-2-yl)phenylimino]ethyl}-pyridin-2-yl)ethylidene]amine (**12**) was 9.40 g (94%) as a pale yellow solid. ^{1}H NMR (500 MHz, C_6D_6, TMS): δ 1.10 (s, 12H, Me), 2.04 (s, 6H, Me), 2.20 (s, 3H, Me), 2.24 (s, 3H, Me), 6.90 (s, 2H, Arom-H), 7.15 (m, 1H, Arom-H), 7.20 (m, 1H, Arom-H), 7.30 (t, $^3J_{HH}$ = 8.0 Hz, 1H, Py-H), 7.80 (s, 1H, Arom-H), 7.90 (s, 1H, Arom-H), 8.45 (d, $^3J_{HH}$ = 8.0 Hz, 1H, Py-H), 8.50 (d, $^3J_{HH}$ = 8.0

Hz, 1H, Py-H). ^{13}C NMR (500 MHz, C_6D_6, (selected signals)): δ 166.96 (C═N), 167.18 (C═N). Anal. Calcd for $C_{29}H_{33}BBrN_3O_2$ (MW: 546.31): C, 63.76; H, 6.09; N, 7.69. Found: C, 63.82; H, 6.18; N, 7.79.

[1-(6-{1-[3-(4,4,5,5-Tetramethyl[1,3,2]dioxaborolan-2-yl)-phenylimino]ethyl}pyridin-2-yl)ethylidene](2,4,6-trimethylphenyl)amine (14). A 5.76 g (0.0205 mol) sample of 1-{6-[1-(2,4,6-trimethylphenylimino)ethyl]pyridin-2-yl}ethanone (**9**), 5.00 g (0.0228 mol) of 3-(4,4,5,5-tetramethyl[1,3,2]dioxaborolan-2-yl)phenylamine (**13**), 100 mL of toluene, and 100 g of fresh molecular sieves were kept at 100 °C for 3 days. The molecular sieves were removed by filtration. The solvent was removed in a rotary evaporator, and the residue was recrystallized from 10 mL of ethanol. The yield of [1-(6-{1-[3-(4,4,5,5-tetramethyl[1,3,2]dioxaborolan-2-yl)phenylimino]-ethyl}pyridin-2-yl)ethylidene](2,4,6-trimethylphenyl)amine (**14**) was 8.70 g (88%) as a pale yellow solid. ^{1}H NMR (500 MHz, C_6D_6, TMS): δ 1.05 (s, 12H, Me), 2.10 (s, 6H, Me), 2.30 (s, 3H, Me), 2.35 (s, 3H, Me), 2.40 (s, 3H, Me), 6.93 (s, 2H, Arom-H), 7.20 (m, 1H, Arom-H), 7.25 (m, 1H, Arom-H), 7.34 (t, $^3J_{HH}$ = 8.0 Hz, 1H, Py-H), 7.91 (s, 1H, Arom-H), 7.98 (s, 1H, Arom-H), 8.40 (d, $^3J_{HH}$ = 8.0 Hz, 1H, Py-H), 8.55 (d, $^3J_{HH}$ = 8.0 Hz, 1H, Py-H). ^{13}C NMR (500 MHz, C_6D_6, (selected signals)): δ 166.96 (C═N), 167.18 (C═N). Anal. Calcd for $C_{30}H_{36}BN_3O_2$ (MW: 481.44): C, 74.84; H, 7.54; N, 8.73. Found: C, 74.96; H, 7.55; N, 8.75.

[1-(6-{1-[4-(4,4,5,5-Tetramethyl[1,3,2]dioxaborolan-2-yl)-phenylimino]ethyl}pyridin-2-yl)ethylidene](2,4,6-trimethylphenyl)amine (17). A 3.20 g (0.0114 mol) sample of 1-{6-[1-(2,4,6-trimethylphenylimino)ethyl]pyridin-2-yl}ethanone (**9**), 2.50 g (0.0114 mol) of 4-(4,4,5,5-tetramethyl[1,3,2]dioxaborolan-2-yl)phenylamine (**16**), 100 mL of toluene, and 100 g of fresh molecular sieves were kept at 100 °C for 3 days. The molecular sieves were removed by filtration. The solvent was removed in a rotary evaporator, and the residue was recrystallized from 10 mL of ethanol. The yield of [1-(6-{1-[4-(4,4,5,5-tetramethyl[1,3,2]dioxaborolan-2-yl)phenylimino]-ethyl}pyridin-2-yl)ethylidene](2,4,6-trimethylphenyl)amine (**17**) was 4.62 g (84%) as a pale yellow solid. ^{1}H NMR (500 MHz, Tol-D_8, TMS): δ 1.15 (s, 12H, Me), 2.05 (s, 6H, Me), 2.20 (s, 3H, Me), 2.25 (s, 3H, Me), 2.30 (s, 3H, Me), 6.80 (m, 2H, Arom-H), 7.06 (m, 2H, Arom-H), 7.40 (t, $^3J_{HH}$ = 8.0 Hz, 1H, Py-H), 8.20 (s, 2H, Arom-H), 8.40 (d, $^3J_{HH}$ = 8.0 Hz, 1H, Py-H), 8.50 (d, $^3J_{HH}$ = 8.0 Hz, 1H, Py-H). ^{13}C NMR (500 MHz, Tol-D_8, (selected signals)): δ 166.51 (C═N), 167.97 (C═N). Anal. Calcd for $C_{30}H_{36}BN_3O_2$ (MW: 481.44): C, 74.84; H, 7.54; N, 8.73. Found: C, 75.02; H, 7.59; N, 8.90.

4-Bromo-2,6-dimethylphenyl)[1-(6-{1-[4-(4,4,5,5-tetramethyl-[1,3,2]dioxaborolan-2-yl)phenylimino]ethyl}pyridin-2-yl)ethylidene]amine (18). A 7.10 g (0.0114 mol) sample of 1-{6-[1-(4-bromo-2,6-dimethylphenylimino)ethyl]pyridin-2-yl}ethanone (**10**), 5.0 g (0.0228 mol) of 4-(4,4,5,5-tetramethyl-[1,3,2]dioxaborolan-2-yl)phenylamine (**16**), 100 mL of toluene, and 100 g of fresh molecular sieves were kept at 100 °C for 3 days. The molecular sieves were removed by filtration. The solvent was removed in a rotary evaporator, and the residue was recrystallized from 10 mL of ethanol. The yield of (4-bromo-2,6-dimethylphenyl)[1-(6-{1-[4-(4,4,5,5-tetramethyl[1,3,2]dioxaborolan-2-yl)phenylimino]ethyl}-pyridin-2-yl)ethylidene]amine (**18**) was 8.20 g (73%) as a pale yellow solid. ^{1}H NMR (500 MHz, CD_2Cl_2, TMS): δ 1.30 (s, 12H, Me), 2.00 (s, 6H, Me), 2.20 (s, 3H, Me), 2.45 (s, 3H, Me), 6.70 (m, 2H, Arom-H), 7.20 (s, 2H, Arom-H), 7.80 (m, 2H, Arom-H), 7.90 (t, $^3J_{HH}$ = 8.0 Hz, 1H, Py-H), 8.30 (d, $^3J_{HH}$ = 8.0 Hz, 1H, Py-H), 8.45 (d, $^3J_{HH}$ = 8.0 Hz, 1H, Py-H). ^{13}C NMR (500 MHz, CD_2Cl_2, (selected signals)): δ 167.39 (C═N), 168.32 (C═N). Anal. Calcd for $C_{29}H_{33}BBrN_3O_2$ (MW: 546.31): C, 63.76; H, 6.09; N, 7.69. Found: C, 63.91; H, 6.20; N, 7.83.

[1-(6-{1-[2-(4,4,5,5-Tetramethyl[1,3,2]dioxaborolan-2-yl)-phenylimino]ethyl}pyridin-2-yl)ethylidene](2,4,6-trimethylphenyl)amineiron(II) Chloride (19). A 6.10 g (0.0127 mol) sample of [1-(6-{1-[2-(4,4,5,5-tetramethyl[1,3,2]dioxaborolan-2-yl)phenylimino]ethyl}pyridin-2-yl)ethylidene](2,4,6-trimethylphenyl)-amine (**11**) was dissolved in 50 mL of THF. Then 1.12 g (0.0088 mol) of iron(II) chloride was added in the reaction mixture in one portion. The resultant blue precipitate was filtered after 12 h of stirring, washed twice by 20 mL of pentane, and dried at 1 mm vacuum. Yield of [1-(6-{1-[2-(4,4,5,5-tetramethyl[1,3,2]dioxaborolan-2-yl)phenylimino]ethyl}pyridin-2-yl)ethylidene](2,4,6-trimethylphenyl)amineiron(II) chloride (**19**) was 3.48 g (45%). Anal. Calcd for $C_{30}H_{36}BCl_2FeN_3O_2$ (MW: 608.19): C, 59.25; H, 5.97; N, 6.91. Found: C, 59.34; H, 6.11; N, 7.03. The structure was determined by X-ray analysis.

(4-Bromo-2,6-dimethylphenyl)[1-(6-{1-[2-(4,4,5,5-tetramethyl[1,3,2]dioxaborolan-2-yl)phenylimino]ethyl}pyridin-2-yl)ethylidene]amineiron(II) Chloride (20). A 9.00 g (0.0165 mol) sample of (4-bromo-2,6-dimethylphenyl)[1-(6-{1-[2-(4,4,5,5-tetramethyl[1,3,2]dioxaborolan-2-yl)phenylimino]ethyl}pyridin-2-yl)ethylidene]amine (**12**) was dissolved in 50 mL of THF. Then 1.25 g (0.0099 mol) of iron(II) chloride was added in the reaction mixture in one portion. The resultant blue precipitate was filtered after 12 h of stirring, washed twice by 20 mL of pentane, and dried at 1 mm vacuum. Yield of (4-bromo-2,6-dimethylphenyl)[1-(6-{1-[2-(4,4,5,5-tetramethyl[1,3,2]dioxaborolan-2-yl)phenylimino]ethyl}-pyridin-2-yl)ethylidene]amineiron(II) chloride (**20**) was 3.19 g (48%). Anal. Calcd for $C_{29}H_{33}BBrCl_2FeN_3O_2$ (MW: 673.06): C, 51.75; H, 4.94; N, 6.24. Found: C, 51.92; H, 5.18; N, 6.37.

[1-(6-{1-[3-(4,4,5,5-Tetramethyl[1,3,2]dioxaborolan-2-yl)-phenylimino]ethyl}pyridin-2-yl)ethylidene](2,4,6-trimethylphenyl)amineiron(II) Chloride (21). A 8.00 g (0.0166 mol) amount of [1-(6-{1-[3-(4,4,5,5-tetramethyl[1,3,2]dioxaborolan-2-yl)phenylimino]ethyl}pyridin-2-yl)ethylidene](2,4,6-trimethylphenyl)amine (**14**) was dissolved in 50 mL of THF. Then 1.26 g (0.0099 mol) of iron(II) chloride was added in the reaction mixture in one portion. The resultant blue precipitate was filtered after 12 h of stirring, washed twice by 20 mL of pentane, and dried at 1 mm vacuum. Yield of [1-(6-{1-[3-(4,4,5,5-tetramethyl[1,3,2]dioxaborolan-2-yl)phenylimino]ethyl}pyridin-2-yl)ethylidene](2,4,6-trimethylphenyl)amineiron(II) chloride (**21**) was 4.12 g (68%). Anal. Calcd for $C_{30}H_{36}BCl_2FeN_3O_2$ (MW: 608.19): C, 59.25; H, 5.97; N, 6.91. Found: C, 59.36; H, 6.24; N, 7.08.

[1-(6-{1-[4-(4,4,5,5-Tetramethyl[1,3,2]dioxaborolan-2-yl)-phenylimino]ethyl}pyridin-2-yl)ethylidene](2,4,6-trimethylphenyl)amineiron(II) Chloride (22). A 1.00 g (0.0021 mol) portion of [1-(6-{1-[4-(4,4,5,5-tetramethyl[1,3,2]dioxaborolan-2-yl)phenylimino]ethyl}pyridin-2-yl)ethylidene](2,4,6-trimethylphenyl)amine (**17**) was dissolved in 60 mL of THF. Then 0.25 g (0.0020 mol) of iron(II) chloride was added in the reaction mixture in one portion. The resultant blue precipitate was filtered after 12 h of stirring, washed twice by 20 mL of pentane, and dried at 1 mm vacuum. Yield of [1-(6-{1-[4-(4,4,5,5-tetramethyl[1,3,2]dioxaborolan-2-yl)phenylimino]ethyl}pyridin-2-yl)ethylidene](2,4,6-trimethylphenyl)amineiron(II) chloride (**22**) was 1.04 g (87%). Anal. Calcd for $C_{30}H_{36}BCl_2FeN_3O_2$ (MW: 608.19): C, 59.25; H, 5.97; N, 6.91. Found: C, 59.48; H, 6.14; N, 7.05. The structure was determined by X-ray analysis.

(4-Bromo-2,6-dimethylphenyl)[1-(6-{1-[4-(4,4,5,5-tetramethyl[1,3,2]dioxaborolan-2-yl)phenylimino]ethyl}pyridin-2-yl)ethylidene]amineiron(II) Chloride (23). A 2.00 g (0.00366 mol) amount of (4-bromo-2,6-dimethylphenyl)[1-(6-{1-[4-(4,4,5,5-tetramethyl[1,3,2]dioxaborolan-2-yl)phenylimino]ethyl}pyridin-2-yl)ethylidene]amine (**18**) was dissolved in 50 mL of THF. Then 0.41 g (0.0032 mol) of iron(II) chloride was added in the reaction mixture in one portion. The resultant blue precipitate was filtered after 12 h of stirring, washed twice by 20 mL of pentane, and dried

at 1 mm vacuum. Yield of (4-bromo-2,6-dimethylphenyl)[1-(6-{1-[4-(4,4,5,5-tetramethyl[1,3,2]dioxaborolan-2-yl)phenylimino]ethyl}-pyridin-2-yl)ethylidene]amineiron(II) chloride (**23**) was 1.96 g (90%). Anal. Calcd for $C_{29}H_{33}BBrCl_2FeN_3O_2$ (MW: 673.06): C, 51.75; H, 4.94; N, 6.24. Found: C, 51.93; H, 5.19; N, 6.31.

General Conditions of the Oligomerizations. Ethylene oligomerizations are done in a 1 L stainless steel Autoclave Engineers Zipperclave. Catalyst and cocatalyst are charged separately using stainless steel injection tubes. The complexes **1**, **19**, **20**, **21**, **22**, and **23** are activated by modified methylaluminoxane (MMAO). The steps for a typical oligomerization are as follows. The injectors are charged in a glovebox. The cocatalyst is obtained as a 7 wt % solution in *o*-xylene and is charged as such into the injector assembly along with a 10 mL chase of *o*-xylene. The catalysts are prepared as suspensions in *o*-xylene (10 mg/100 mL). A sample is pulled from a well-stirred suspension and is added to a 10 mL charge of *o*-xylene. The injectors are attached to autoclave ports equipped with dip tubes. Nitrogen is sparged through the loose fittings at the attachment points prior to making them tight. The desired charge of *o*-xylene is then pressured into the autoclave. The agitator and heater are turned on. When the desired temperature is reached, the cocatalyst is charged to the clave by blowing ethylene down through the cocatalyst injector. After a significant pressure rise is seen in the autoclave to indicate the cocatalyst and chase solvent have entered, the injector is isolated from the process using its valves. The pressure controller is then set to 5 psig below the desired ethylene operating pressure and is put in the automatic mode to allow it to control the operation of the ethylene addition valve. When the pressure is 5 psig below the desired operating pressure, the controller is put into manual mode and the valve is set to 0% output. When the batch temperature is stable at the desired value, the catalyst is injected using enough nitrogen such that the reactor pressure is boosted to the desired pressure. At the same time as the catalyst injection, the pressure controller is put in the automatic mode and the oligomerization is started. The 5 psi boost is obtained routinely by having a small reservoir between the nitrogen source and the catalyst injector. A valve is closed between the nitrogen source and the reservoir prior to injecting the catalyst so the same volume of nitrogen is used each time to inject the catalyst suspension. To stop the oligomerization, the pressure controller is put into manual, the ethylene valve is closed, and the reactor is cooled. The reaction time is 1 h.

X-Ray Diffraction Studies. Data for all structures were collected using a Bruker CCD system at −100 °C. Structure solution and refinement were performed using the Shelxtl[14] set of programs. The Platon-Squeeze[15] program was used to correct the data where the solvent molecules could not be correctly modeled.

Acknowledgment. The authors wish to thank Kurt Adams for funding the X-ray research.

Supporting Information Available: Crystallographic information (CIF file) for compounds **1**, **3**, **19**, **21**, **22**, and **23**. These materials are available free of charge via the Internet at http://pubs.acs.org.

OM800036B

(14) Sheldrick, G. *Shelxtl Software Suite*, *Version 5.1*;Bruker AXS Corp.: Madison, WI., 1997.

(15) Spek A. L. *PLATON*, *A Multipurpose Crystallographic Tool*; Utrecht University: Utrecht, The Netherlands, 2005.